

Pressure effects on the electronic structure and superconducting critical temperature of Li_2B_2

E. Martínez-Guerra¹, F. Ortiz-Chi², S. Curtarolo³ and R. de Coss²

¹ Facultad de Ciencias Físico-Matemáticas, Universidad Autónoma de Nuevo León, Ciudad Universitaria 66450, San Nicolás de los Garza, N.L., México

² Departamento de Física Aplicada, Centro de Investigación y de Estudios Avanzados del I.P.N., Cordemex 97310, Mérida, Yucatán, México

³ Department of Mechanical Engineering and Materials Science, Duke University, Hudson Hall 27708, Durham, North Carolina, USA

E-mail: edgar.martinezgrr@uanl.edu.mx

Abstract. We present the structural, electronic and superconducting properties of Li_2B_2 under pressure within the framework of the density functional theory. The structural parameters, electronic band structure, phonon frequency of the E_{2g} phonon mode and superconducting critical temperature T_c were calculated for pressures up to 20 GPa. We predicted that the superconducting critical temperature of Li_2B_2 is about 11 K and this decreases as pressure increases. We found that even though the lattice dynamics of the E_{2g} phonon mode is similar to MgB_2 , the reduction of the σ -band density of states at Fermi level and the raising of the E_{2g} phonon frequency with pressure were determinant to decrease λ and consequently T_c .

PACS numbers: 74.25.Jb, 74.62.Fj, 74.70.Ad

Submitted to: *J. Phys.: Condens. Matter*

1. Introduction

High T_c superconductivity in intermetallic layered structures attracted much attention since the discovery of superconductivity in magnesium diboride (MgB_2) in 2001 [1]. However, MgB_2 keeps being the intermetallic material with the highest superconducting temperature (39 K) and even is well known that this property is based on the strong coupling of its covalent B sigma bands with B bond-stretching modes [2, 3, 4, 5, 6, 7], it has not been possible to predict a new diboride type to enhance it. On the other hand, it is widely accepted that the superconductivity on intercalated systems as CaC_6 is dominated by the interaction of free-electron-like interlayer states with soft intercalant modes. Lately, in this context, new proposals for the quest of layered intercalated superconductors are being merged. The most recent theoretical study reports that, by

decorating graphene with Li atoms, a superconductor at a much higher temperature with respect to Ca-covered graphene is obtained [10]. The Li-Be layered compounds with a low-dimensional electronic structure and strong electron-phonon (e-ph) coupling, are another family of Li-based compounds with possible superconducting properties under high pressure [11, 12]. More recently, there has been considerable interest in the structural stability, electronic band structure and chemical bond of Li-B compounds under high pressures [13, 14, 15].

Layered Li-based materials with a quasi-two-dimensional electronic structure and high dynamical energy scales resulting from the Li-atom motion are potential candidates for high T_c superconductors. In that direction, first-principles calculations using data-mining approach have predicted new hypothetical intermetallic materials [16, 17] called metal-sandwich (MS) structures MS1(MB) and MS2(M_2B_2), which also have sp_2 -layers of boron as in MgB_2 but separated by two metal layers M [16]. Particularly, LiB and Li_2B_2 resulted marginally stable under ambient conditions and they become favored over the known stoichiometric compounds under pressure [16, 17]. Both compounds resulted remarkably interesting since the σ - and π -bands derived from its boron p_{xy} - and p_z -orbitals were similars to those in MgB_2 [7, 18, 19] and therefore a similar superconductor mechanism based on the electron-phonon coupling between the σ - and π -bands and the E_{2g} phonon mode in the boron planes was expected.

Recent calculations revealed that the electron-phonon coupling (λ) in Li_2B_2 was weaker than in MgB_2 , estimated about 0.57 [19] in comparison to those reported for magnesium diboride ranging from 0.61 to 1.1 [2, 3, 7, 20, 21, 22, 23]. Thus, the transition temperature of Li_2B_2 was reported to be around 7 K [19]. Now it is also widely accepted that in MgB_2 the electron-phonon coupling take a large contribution from σ -bands but also a small participation from π -bands[23, 24]. Therefore the seemingly unimportant π -electrons at ϵ_F could be determinant to increase the transition temperature of Li_2B_2 . Thus, an appropriate doping of Li_2B_2 , in which π -electrons are increased, could result in a higher T_c than in MgB_2 . This hypothesis was tested by Calandra *et al.* [18] substituting Li atoms with Mg or Al. Nevertheless, the tests showed that it was difficult to induce a significant amount of π -states at ϵ_F with small doping because the band crossing in Li_2B_2 happens to be exactly at ϵ_F , around 2 eV lower than in MgB_2 [7]. Furthermore, even from a thermodynamical stand point, doping Li_2B_2 might be as difficult as it is for MgB_2 [8].

From the McMillan equation [37] (Eq. 2), Li_2B_2 would be optimistic compared to MgB_2 , because Li_2B_2 (0.48 states/eV) has a higher density of states of B atoms than MgB_2 (0.39 states/eV) at ϵ_F and this could enhance the electron-phonon coupling constant. However, this is not enough for arising T_c . One interesting case is represented by CaBeSi [9], a material with σ - and π -bands at the Fermi level and density of states twice higher than in MgB_2 , but with a very low critical temperature $T_c=0.4$ K. Thus, while the band structure can present strong similarities with both σ - and π -bands crossing the Fermi level, the phonon structure and the e-ph interaction could differ substantially.

In this paper, we have analyzed why the T_c of Li_2B_2 (7 K) has been reported lower than for MgB_2 (39 K) and if it was possible to enhance the e-ph coupling of Li_2B_2 and consequently, the superconducting temperature by applying hydrostatic pressure. Since the in-plane motion of the boron atoms changes the boron orbitals overlap, an important electron-phonon coupling could be expected mainly for the σ - bands at ϵ_F and the E_{2g} phonon mode. After a careful analysis of the pressure effects on the band structure and the E_{2g} phonon frequency, we found that the electron-phonon coupling and T_c decrease with pressure as a result of the strong reduction of the boron- p_{xy} states contribution to the density of states at Fermi level and the hardening of the E_{2g} phonon frequency as pressure was applied.

2. COMPUTATIONAL DETAILS

We studied the Li_2B_2 compound (crystal structure: MS2) as model of layered lithium borides. Li_2B_2 has eight atoms in the primitive unit cell and a space group $\text{P6}_3/\text{mmc}$ (No.194). Wickoff positions: Li1(4f) $(\frac{1}{3}, \frac{2}{3}, \frac{1}{4} - \frac{z}{4})$, B1(2b) $(0, 0, \frac{1}{4})$ and B2(2d) $(\frac{1}{3}, \frac{2}{3}, \frac{3}{4})$, see Fig. 1. The structural parameters were fully relaxed through a molecular dynamics scheme: $a=b=3.087 \text{ \AA}$, $c=11.18 \text{ \AA}$; $\alpha=\beta=90^\circ$, $\gamma=120^\circ$.

The total energy calculations were performed with SIESTA (Spanish Initiative for Electronic Simulations with Thousands of Atoms) code [25, 26] based on density functional theory with exchange-correlation functionals as parametrized by Perdew, Burke, and Ernzerhof [27] for the generalized gradient approximation (GGA) [28, 29, 30, 31]. This code is implemented with pseudopotentials to describe electron-ion interactions and numerical atomic orbitals to expand the valence wavefunctions. Pseudopotentials were generated according to the Troullier-Martins procedure [32] using the atomic configurations $1s^2 2s^1$ for Li and $1s^2 2s^2 2p^1$ for B with a core radii of 2.49 and 1.24 atomic units (a.u.) for Li and B, respectively. As the basis set for the valence wavefunctions we have employed a double- ξ basis. To calculate the integrals of the Kohn-Sham hamiltonian, we have used a \mathbf{k} -space sampling via the Monkhorst-Pack matrix $(70 \times 70 \times 70)$ with a meshcutoff of 280 Ry [33]. All calculations were numerically converged when interatomic forces were less than 0.1 meV/\AA .

Li_2B_2 phase was calculated as a function of cell volume V and c/a ratio. We performed total energy calculations for fifteen volumes and seven c/a ratios in order to optimize both. Subsequently, the total energy was fitted to the Murnaghan equation of state [34] to obtain the equilibrium volume (V_0) and the $P - V$ equation of state (EOS). Thus, from the $P - V$ EOS the unit cell volume and c/a ratio were estimated from 0-20 GPa. The E_{2g} -phonon mode was calculated using the frozen-phonon model [35] that, even is a very simple model, it is still a suitable and useful approach [10]. This approach is a direct method in which the distorted Li_2B_2 is treated as a crystal of a lower symmetry than the non-distorted Li_2B_2 . Thus, total energy calculations of distorted crystals were performed to simulate the dynamics of the E_{2g} phonon mode.

The oscillating pattern of the E_{2g} mode corresponds to boron ions in opposite

directions along x - or y -axis, with Li ions stationary (Fig. 2). For this, we have simulated the E_{2g} -phonon mode as a composition of two modes: $E_{2g}(a)$ and $E_{2g}(b)$. Figure 2 represents the vibration pattern of these modes. To implement the displacement pattern of these modes, we defined an adimensional distortion parameter u/a related to the boron bond, where u is the magnitude of the distortion and a the in-plane lattice parameter, using the unit cell volume and c/a ratio for 0, 10 and 20 GPa previously optimized. These distortions simulated expansions and contractions of E_{2g} phonon mode as a function of the u parameter. Thus, to calculate the effective potential due to boron atoms oscillation we use a maximum adimensional displacement of $|u/a|=0.04$ and steps of $\Delta=0.01$. Eight different displacements were calculated to simulate the vibrational dynamics of the $E_{2g}(a)$ and $E_{2g}(b)$ component modes and the total energy values of these configurations were subtracted to the total energy of non-distorted Li_2B_2 when its boron atoms are on its equilibrium positions. The energy differences determined the restitutive potential of each oscillator and they were used to solve numerically the Schrödinger equation and obtain the characteristic frequency of each mode.

The superconducting critical temperature of Li_2B_2 under pressure was evaluated using the McMillan's relation [37],

$$T_c = \frac{\omega}{1.2} \exp \left[\frac{-1.04(1 + \lambda_\sigma)}{\lambda_\sigma - \mu^*(1 + 0.62\lambda_\sigma)} \right], \quad (1)$$

where λ_σ is the coupling constant between σ -band and the E_{2g} mode, ω is the average frequency of the $E_{2g}(a)$ and $E_{2g}(b)$ component modes and μ^* is an adimensional empirical value which represents the repulsive force between Cooper pairs. To determine the coupling constant (λ_σ) quantitatively, we evaluated the deformation potential (D) for $E_{2g}(a)$ and $E_{2g}(b)$ modes under each distortion and used the isotropic limit from the Eliashberg theory [36] with the McMillan's formula [37],

$$\lambda_\sigma = N_B(\epsilon_F) \left[\frac{\hbar^2}{M\omega^2} \right] D^2, \quad (2)$$

where, ω^2 , D , $N_B(\epsilon_F)$ and M are the average of the phonon frequency of the $E_{2g}(a)$ and $E_{2g}(b)$ modes, the deformation potential of the σ -band due to E_{2g} mode, the density of states of boron atoms at Fermi level and total mass of boron atoms inside unit cell, respectively.

3. RESULTS AND DISCUSSION

In Fig. 3, we show the results for the a and c lattice parameters, and the V/V_0 ratio for Li_2B_2 as a function of pressure for $0 \leq P \leq 20$ GPa. It can be seen that a parameter decreases from 3.087 to 3.071 Å while c parameter from 11.187 to 8.0 Å in the range of 20 GPa. Although both, a and c parameters decreases, it is important to note that the slope for c parameter as a function of pressure is higher than for a parameter, that is, it would be easier to compress Li_2B_2 through z -direction than in plane direction. Conversely, V/V_0 decreases non-linearly and Li_2B_2 could be compressed about 30% when it is applied over 20 GPa.

Table 1. Mulliken populations of valence orbitals of B and Li.

Atom	Pressure [GPa]	Q	s	p_x	p_y	p_z	d
Li	0	1.021	0.334	0.256	0.256	0.175	-
	10	1.070	0.381	0.279	0.279	0.131	-
	20	1.180	0.461	0.299	0.299	0.120	-
B	0	5.957	1.819	1.459	1.459	0.999	0.218
	10	5.859	1.835	1.441	1.441	0.930	0.213
	20	5.641	1.765	1.366	1.366	0.958	0.185

The band structure of MgB_2 and Li_2B_2 are shown in Fig. 4. Both structures are as similar as it was reported before [18, 19]. Li_2B_2 presents the π - and σ -bands which are coupled with E_{2g} phonon mode to induce superconductivity in MgB_2 . However, in Li_2B_2 the sigma band is shifted up by 0.23 eV and the pi-band is shifted down by 1.31 eV, with respect to MgB_2 . This shifting produces that the π - π^* crossing occurs practically at Fermi level, resulting in a small density of states from π -band at ϵ_F . Hence, to evaluate the effects of pressure on the electronic band structure, in Fig. 5 the evolution of the σ - and π -bands with pressure is shown. From that, it can be observed the energy position relative to ϵ_F of the σ - bands at Γ (E_Γ) and π -bands at K (E_K) as a function of pressure. These results demonstrate that both energies, E_Γ and E_K , decrease as pressure increases. In particular, E_Γ changes from 1.03 eV at 0 GPa to 0.21 eV at 20 GPa, and E_K changes from 0.11 eV at 0 GPa to -0.56 eV at 20 GPa. To provide an explanation of the energy changes of σ - and π -bands in terms of the charge redistribution induced by the pressure, we estimated the charge population of the valence orbitals by using Mulliken populations [38], as shown on Table 1. A charge transfer from B to Li atoms is observed. The B- p_{xy} and B- p_z orbitals loose charge, transferring it to the Li orbitals, mainly to Li- s orbital. It should be pointed out that the values provided in the Mulliken analysis are strongly dependent on the basis set, but trends observed in the charge transfer process are reliable.

The total and partial density of states of B, B- p_{xy} and B- p_z orbitals as a function of pressure inside unit cell are shown in Fig. 6. From that, it is clear that at 0 GPa the main contribution at ϵ_F is coming from the σ -band. For 0 GPa, the contributions of the B- p_{xy} and B- p_z orbitals to the density of states (DOS) at ϵ_F are 0.35 and 0.075 states/eV, respectively. We find that pressure induce a strong reduction of the B- p_{xy} and B- p_z orbitals contribution to the DOS at ϵ_F . Thus, pressure of 20 GPa induces a reduction of 50% and 37% in the B- p_{xy} and B- p_z orbitals contributions, respectively, with respect to the 0 GPa pressure values. These results are summarized on Table 2. From these results, we find that the behavior of the σ - and π -bands with pressure correlates with the charge transfer and the reduction of states at Fermi level of the partial DOS corresponding to the B- p_{xy} and B- p_z orbitals. Thus, as the coupling constant λ is directly proportional to

Table 2. Density of states at ϵ_F for B- p_{xy} and B- p_z orbitals at the calculated lattice constants at 0, 10 and 20 GPa.

Pressure [GPa]	B(p_{xy}) [states/eV]	B(p_z) [states/eV]
0	0.352	0.075
10	0.271	0.036
20	0.178	0.028

$N_B(\epsilon_F)$ and this one is weighted by contributions of B- p_{xy} and B- p_z , the present result did not represent an advance in our quest to increase λ in comparison with MgB_2 . From Eq. (2), we can see that the other parameters controlling λ and therefore T_c are: the phonon frequency $\omega[E_{2g}]$ and the deformation potential D .

To further investigate E_{2g} phonon frequency value, in Fig. 7 is plotted the energy as the atoms are displaced by an adimensional amount u/a according to $E_{2g}(a)$ and $E_{2g}(b)$ modes. Usually, phonons are harmonic for small displacements of the atoms with respect to equilibrium, but anharmonic behavior is observed for large displacements. A different source of anharmonicity take place for atomic displacement patterns with non symmetric atomic environment, that is, for the cases when the atom experiences a different force field for positive and negative displacements with respect to the equilibrium position. Thus, in the present case, we find that the total-energy as a function of the distortions for the $E_{2g}(a)$ and $E_{2g}(b)$ phonon modes show an asymmetric and symmetric behavior, respectively (see Fig. 7). For the $E_{2g}(a)$ mode, the distortion energy could be reasonably approximated by the anharmonic relation $E(u/a) = A_2(u/a)^2 + A_3(u/a)^3 + A_4(u/a)^4$. While for the $E_{2g}(b)$ mode, it could be fitted to $E(u/a) = A_2(u/a)^2 + A_4(u/a)^4$. Using the calculated well potential for each pressure and numerically solving the Schrödinger equation, we obtained $\omega[E_{2g}(a)] = 79.48$ meV (641.06 cm^{-1}) when Li_2B_2 is free of pressure and $\omega[E_{2g}(a)] = 93.95$ meV (757.78 cm^{-1}) and $\omega[E_{2g}(a)] = 104.39$ meV (841.98 cm^{-1}) for 10 and 20 GPa, respectively. Therefore, the obtained results show that the hydrostatic pressure causes an increment in $E_{2g}(a)$ phonon frequencies, and the rising does not depend linearly on the increasing pressure. Similarly, we obtained $\omega[E_{2g}(b)] = 83.04$ meV (669.78 cm^{-1}) when Li_2B_2 is non-distorted and $\omega[E_{2g}(b)] = 93.95$ meV (757.78 cm^{-1}) and $\omega[E_{2g}(b)] = 104.78$ meV (845.13 cm^{-1}) for 10 and 20 GPa, respectively. Harmonic and anharmonic frequencies were estimated for $E_{2g}(b)$ mode but they resulted to be equal and linearly dependent of pressure. Thus, because the frequency is directly proportional to the superconducting critical temperature, these relationship could be a good way to enhance T_c .

Despite that, it was quite important to quantify the deformation potential from the in-plane motions of the E_{2g} mode changes the boron orbital overlap and therefore the pairing superconductor. To determine the deformation potential due to vibrations of the $E_{2g}(a)$ and $E_{2g}(b)$ modes phonons, we considered that only σ -band is coupled to E_{2g} phonon, even that in MgB_2 it has been well established that σ - and π -bands are coupled

Table 3. Calculated values of the total density of states of boron atoms inside unit cell at Fermi level $N_B(\epsilon_F)$, the averaged value of the frequencies of the components of the E_{2g} phonon mode $\omega(E_{2g})$, the deformation potential D , and the coupling constant λ_σ .

P[GPa]	$N_B(\epsilon_F)[\frac{\text{states}}{\text{eV}}]$	$\omega(E_{2g})[\text{meV}]$	$D_\sigma[\frac{\text{eV}}{\text{\AA}}]$	λ_σ
0	0.48	81.26	12.88	0.57
10	0.35	93.95	13.17	0.32
20	0.29	104.58	13.21	0.22

Table 4. Estimated values of T_c as a function of pressure for different values of Coulomb repulsion $\mu^* = 0, 0.1$ and 0.14 .

P[GPa]	$\mu^* = 0$	$\mu^* = 0.1$	$\mu^* = 0.14$
0	45	18.6	10.95
10	12	0.98	0.11
20	3.6	0.01	0.07

with the E_{2g} mode. We made this approximation because of two reasons: 1) lackness of π -states, and 2) σ -states are the main contribution to the electron-phonon coupling in MgB_2 [39, 40, 41]. Thus, by estimating the average energy of the σ -band through Γ - A path for each distortion, we determined the deformation potential as suggested by Khan-Allen [42], $D = (1/2)(d\bar{\epsilon}/du)$. As it is shown on Table 3, the deformation potential increased slightly as a result of an increase of electron concentration when pressure arise. However, most remarkably is that average values of D for E_{2g} in 0–20 GPa range are quite close to the reported value of 12.88 eV/Å for MgB_2 [2] and then this contribution would be at least comparable with magnesium diboride.

Finally, we evaluated the electron-phonon coupling λ of the σ -band and the E_{2g} phonon within isotropic limit of the Eliashberg theory with the McMillan's equation and the values of $\omega[E_{2g}]$, $N_B(\epsilon_F)$ and D calculated previously. These results are also shown on Table 3. From these data, it is suggested that the reduced density of states of $B-p_{xy}$ at ϵ_F and the enhanced frequency of the E_{2g} phonon mode are the main causes for the decreasing of λ . To establish a connection between T_c and λ , we considered the strong coupling approach from Eliashberg theory, Eq. 1. By adopting the conventional value of Coulomb repulsion $\mu = 0.14$ and two additional of $\mu^* = 0$ and $\mu^* = 0.1$ [43], we estimated T_c at different pressures. The results are summarized on Table 4. T_c was found to decrease from 45 to 3.6 K with a null Coulomb repulsion, from 18.6 to 0.01 K with $\mu^* = 0.1$ and from 10.95 to 0.07 K with $\mu^* = 0.14$. With all choices of μ^* , the resulting T_c has a continuously reduced trend and practically vanishes at 20 GPa.

4. CONCLUSIONS

In conclusion, we have presented a first-principle investigation of the electronic structure, phonon frequency of the E_{2g} mode, the deformation potential of the σ -band and the electron-phonon coupling λ for Li_2B_2 under pressure from 0–20 GPa within the framework of density functional theory. We predicted a reduction of λ from 0.57 at 0 GPa to 0.22 at 20 GPa. Even the lattice dynamics of the E_{2g} phonon mode resulted similar to MgB_2 , the reduced density of states of B- p_{xy} at Fermi level and the raising of the phonon frequency corresponding to the E_{2g} mode with pressure were determinant to decrease λ and consequently T_c .

5. Acknowledgments

One of the authors (E.M.G.) gratefully acknowledges financial support from the Consejo Nacional de Ciencia y Tecnología (CONACYT-México) through a posdoctoral scholarship (No. 55171). Also, E.M.G. would like to thank to Ramiro Quijano Quiñones and Omar de la Peña Seaman for technical assistance and useful discussions. This research was partially funded by CONACYT-México under Grant No. 83630 and No. 133022.

References

- [1] Nagamatsu J, Nakagawa N, Muranaka T, Zenitani Y and Akimitsu J 2001 *Nature* **410** 63
- [2] An J M and Pickett W E 2001 *Phys. Rev. Lett.* **86** 4366
- [3] Kortus J, Mazin I I, Belashchenko K D, Antropov V P and Boyer L L 2001 *Phys. Rev. Lett.* **86** 4656
- [4] Baron A Q R, Uchiyama H, Tsusui S, Tanaka Y, Ishikawa D, Sutter J P, Lee S, Tajima S, Heid R and Bhonen K P 2007 *Physica C* **456** 83
- [5] Floris A, Sanna A, Lüders M, Profeta G, Lathiotakis N N, Marques M A L, Franchini C, Gross E K U, Continenza A and Massidda S 2007 *Physica C* **456** 45
- [6] Kortus J 2007 *Physica C* **456** 54
- [7] de la Peña O, Aguayo A and de Coss R 2002 *Phys. Rev. B* **66** 012511
- [8] Chepulsikii R V and Curtarolo S 2009 *Phys. Rev. B* **79** 134203
- [9] Bersier C, Floris A, Sanna A, Profeta G, Continenza A, Gross E K U and Massidda A 2009 *Phys. Rev. B* **79** 104503
- [10] Profeta G, Calandra M and Mauri F 2012 *Nat. Phys.* **8** 131
- [11] Feng J, Henning RG, Ashcroft NW and Hoffmann R 2008 *Nature* **451** 445
- [12] Xu Y, Chen C and Wu B 2012 *Solid State Commun.* **152** 151
- [13] Hermann A, Suarez-Alcubilla A, Gurtubay IG, Yang LM, Bergara A, Ashcroft NW and Hoffmann R 2012 *Phys. Rev. B* **86** 144110
- [14] Hermann A, McSorley A, Ashcroft NW and Hoffmann R 2012 *J. Am. Chem. Soc.* **134** 18606
- [15] Peng F, Miao M, Wang H, Li Q and Ma Y 2012 *J. Am. Chem. Soc.* **134** 18599
- [16] Kolmogorov A N and Curtarolo S 2006 *Phys. Rev. B* **73** 180501(R)
- [17] Kolmogorov A N and Curtarolo S 2006 *Phys. Rev. B* **74** 224507
- [18] Calandra M, Kolmogorov A N and Curtarolo S 2007 *Phys. Rev. B* **75** 144506
- [19] Liu A Y and Mazin I I 2007 *Phys. Rev. B* **75** 064510
- [20] Wang Y, Plackowski T and Junod A 2001 *Physica C* **355** 179

- [21] Bouquet F, Fisher R A, Phillips N E, Hinks D G and Jorgensen J D 2001 *Phys. Rev. Lett.* **87** 047001
- [22] Yildirim T, Gülseren O, Lynn J W, Brown C M, Udovic T J, Huang Q, Rogado N, Regan K A, Hayward M A, Slusky J S, He T, Hass M K, Khalifah P, Inumaru K and Cara R J 2001 *Phys. Rev. Lett.* **87** 037001
- [23] Choi H J, Roundy D, Sun H, Cohen M L and Louie S G 2002 *Nature* **418** 758
- [24] De la Peña-Seaman O, de Coss R, Heid R, and Bohnen KP 2010 *Phys. Rev. B* **82** 224508
- [25] Soler J M, Artacho E, Gale J D, García A, Junquera J, Ordejón P and Sánchez Portal D 2002 *J. Phys.: Condens. Matter* **14** 2745
- [26] Ordejón P, Artacho E and Soler J M 1996 *Phys. Rev. B* **53** 10441
- [27] Perdew J P, Burke K and Ernzerhof M 1996 *Phys. Rev. Lett.* **77** 3865
- [28] Langreth D C and Mehl M J 1983 *Phys. Rev. B* **28** 1809
- [29] Becke A D 1988 *Phys. Rev. A* **38** 3098
- [30] Perdew J P, Chevary J A, Vosko S H, Jackson K A, Pederson M R, Singh D J and Fiolhais C 1992 *Phys. Rev. B* **46** 6671
- [31] Perdew J P, Chevary J A, Vosko S H, Jackson K A, Pederson M R, Singh D J and Fiolhais C 1993 *Phys. Rev. B* **48** 4978(E)
- [32] Troullier N and Martins J L 1991 *Phys. Rev. B* **43** 1993
- [33] Monkhorst H J and Pack J D 1976 *Phys. Rev. B* **13** 5188
- [34] Murnaghan D F 1944 *Proc. Natl. Acad. Sci. USA* **30** 244
- [35] Kunc K and Martin R M 1983 *Physica B&C* **117** 511
- [36] Eliashberg G M 1960 *Sov. Phys. JETP* **11** 696
- [37] McMillan W L 1968 *Phys. Rev.* **167** 331
- [38] Mulliken R S 1955 *J. Chem. Phys.* **23** 1833
- [39] Kong Y, Dolgov O V, Jepsen O and Andersern O K 2001 *Phys. Rev. B* **64** 020501(R)
- [40] Liu A Y, Mazin I I and Kortus J 2001 *Phys. Rev. Lett.* **87** 087005
- [41] Golubov A A, Kortus J, Dolgov O V, Jepsen O, Kong Y, Andersen O K, Gibson B J, Ahn K and Kremmer R K 2002 *J. Phys.: Condens. Matter* **14** 1353
- [42] Khan F S and Allen P B 1984 *Phys. Rev. B* **29** 3341
- [43] de la Peña-Seaman O, de Coss R, Heid R, and Bohnen K.P. 2007 *J. Phys.: Condens. Matter* **19** 476216

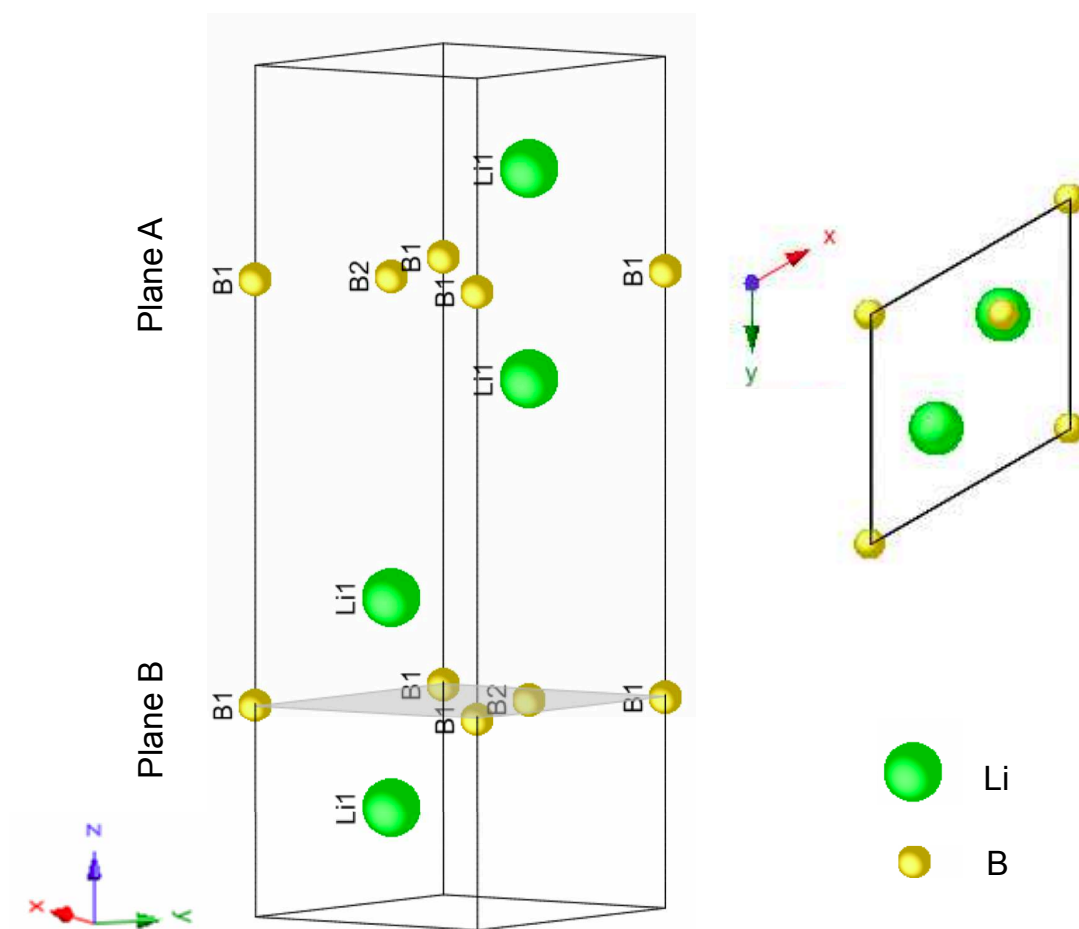


Figure 1. a) Crystal structure of Li_2B_2 (3D view). b) Hexagonal layers of boron (yellow) are separated by triangular layers of lithium (green) (2D view).

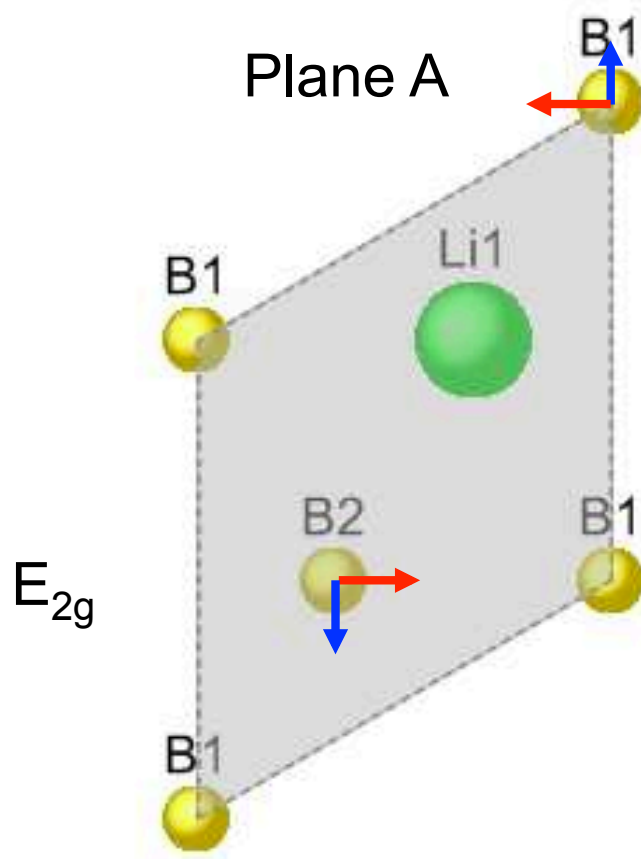


Figure 2. Vibration patterns of the components of the E_{2g} mode. a) $E_{2g}(\text{a})$ and b) $E_{2g}(\text{b})$ modes.

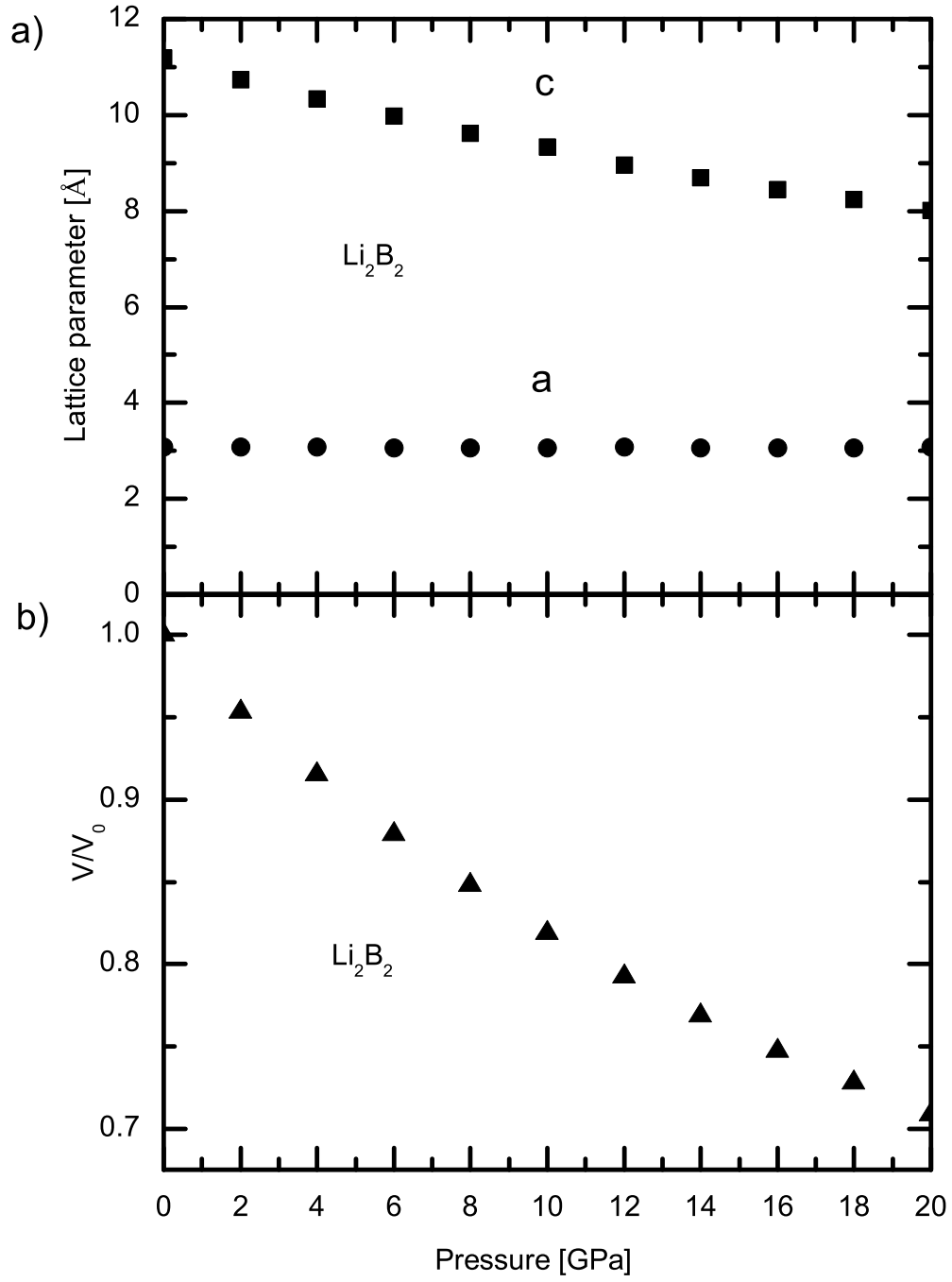


Figure 3. Structural parameters of Li_2B_2 as a function of pressure. a) a and c lattice parameters and b) V/V_0 ratio.

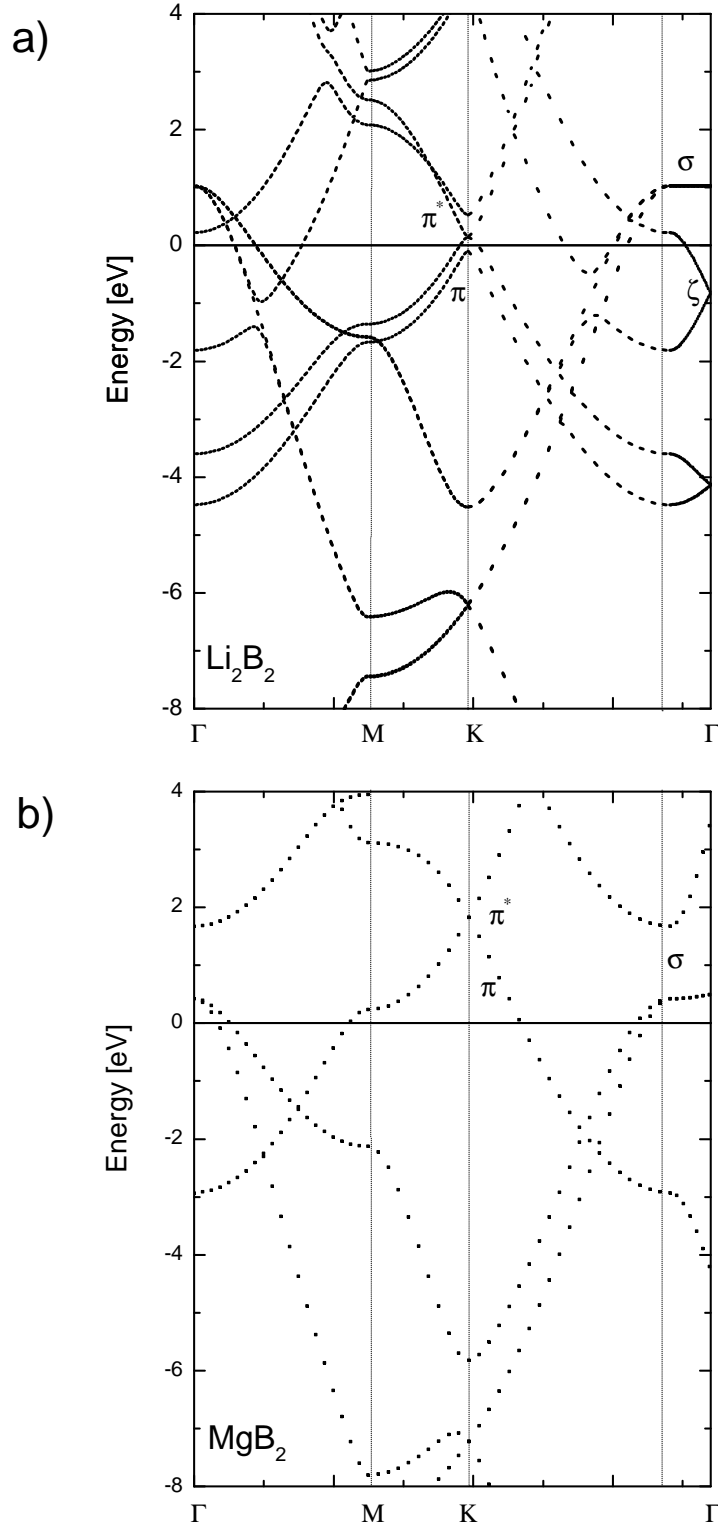
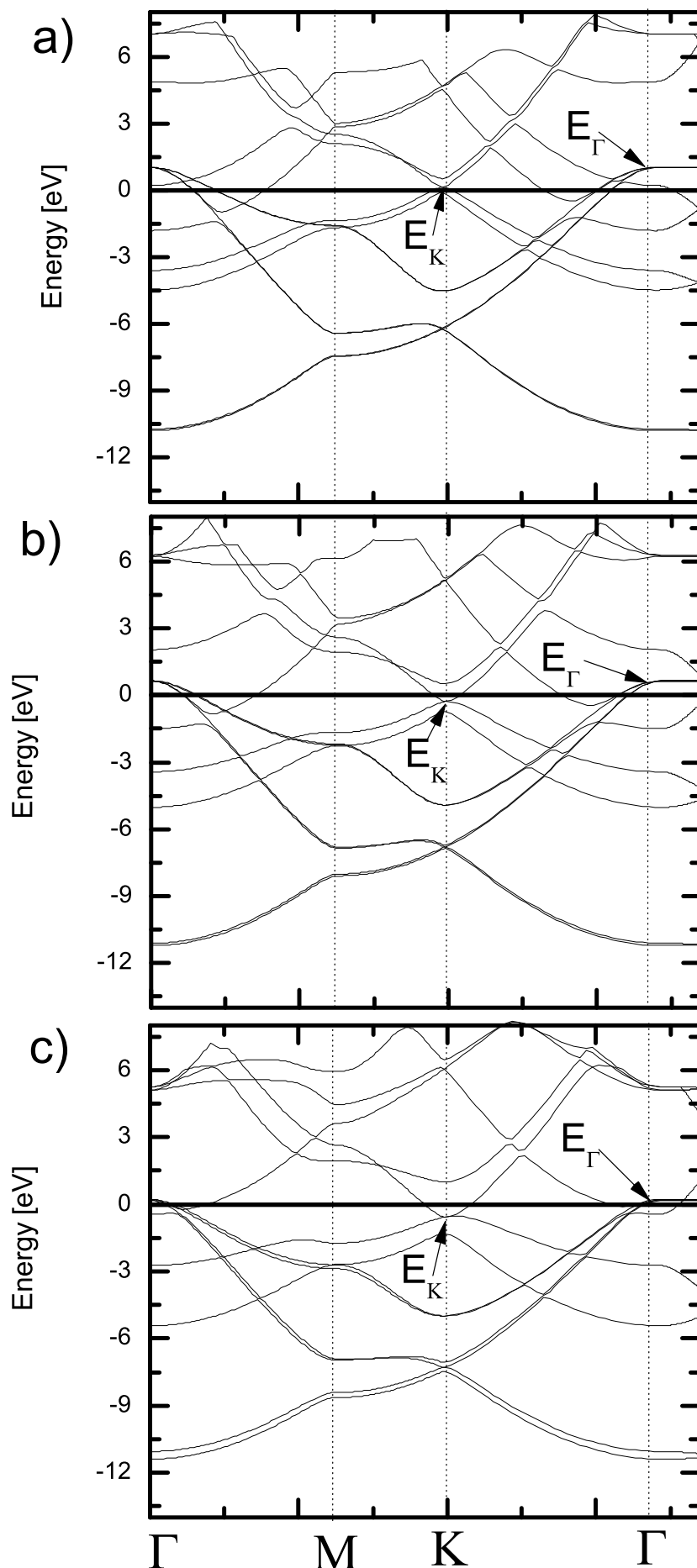


Figure 4. Electronic band structure at the calculated equilibrium lattice constants for a) Li_2B_2 and b) MgB_2 .



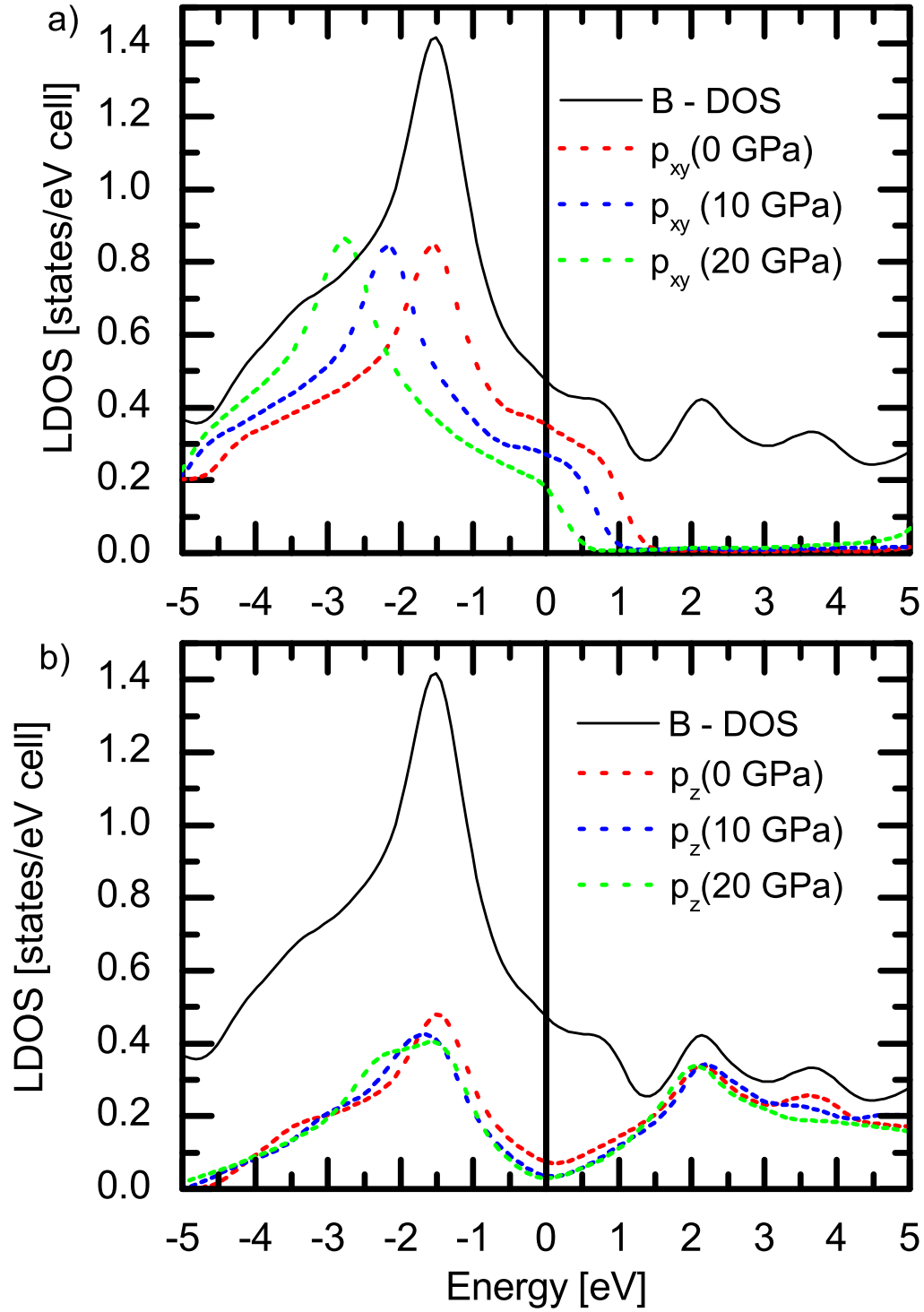


Figure 6. Local and partial density of states of boron atoms in Li_2B_2 for 0, 10 and 20 GPa. a) Partial density of states of B- p_{xy} orbitals inside unit cell and b) partial density of states of B- p_z orbitals inside unit cell.

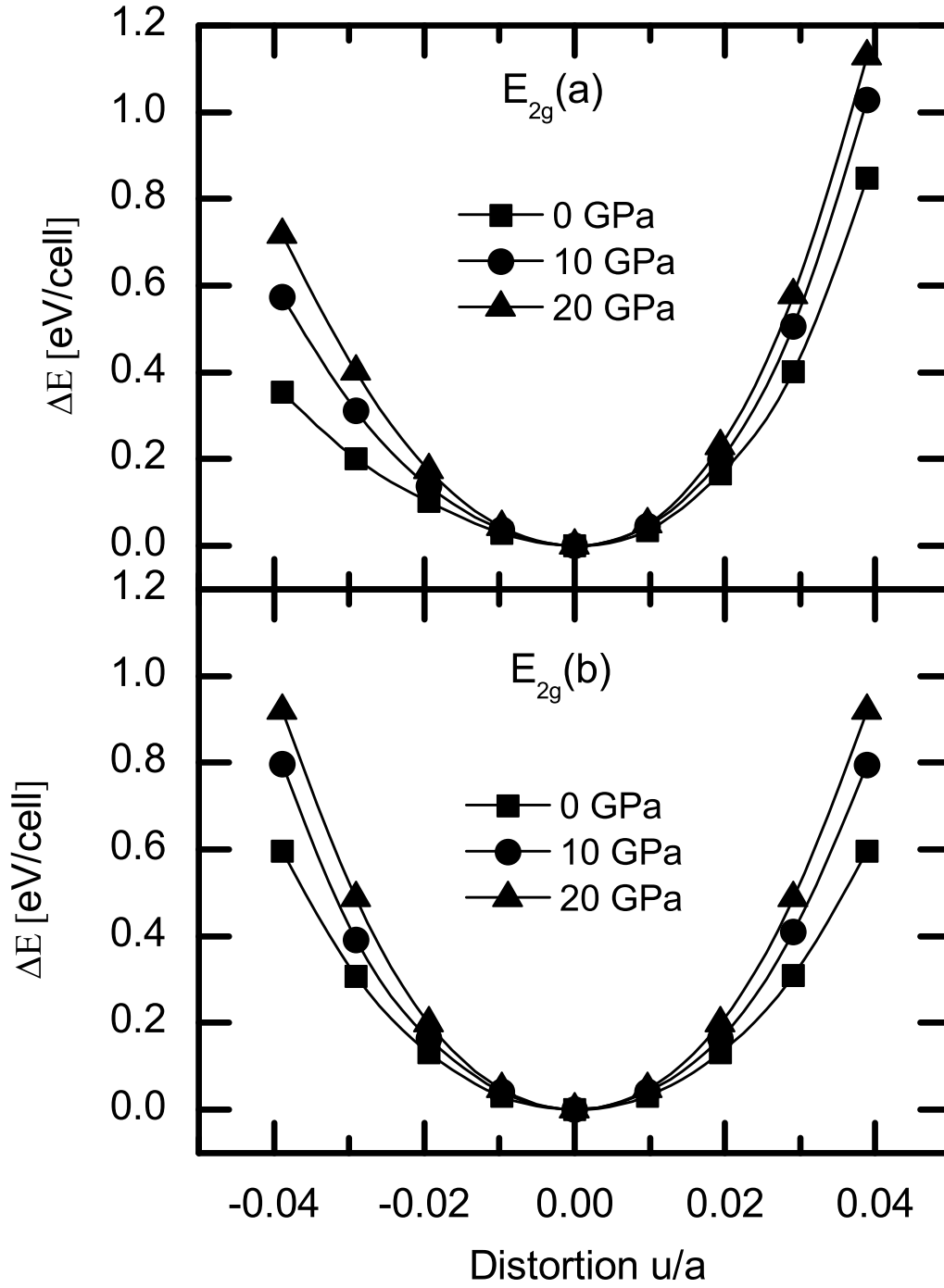


Figure 7. Total energy as a function of boron displacements for the E_{2g} mode. The $E_{2g}(a)$ boron in-plane mode (top) is strongly anharmonic while the $E_{2g}(b)$ (bottom) is practically harmonic.